

Theory of phonoritons and experiments to determine phonoriton dispersion and spectrum

Bing Shen Wang and Joseph L. Birman

Department of Physics, City College of CUNY, New York, New York 10031

(Received 24 May 1990)

Under intense excitation by an electromagnetic wave near the exciton resonance, the exciton-polariton spectrum around the frequencies of the Stokes and anti-Stokes scattered polaritons will be modified by certain phonons via the exciton-phonon interaction, producing new elementary excitations called "phonoritons" (A. L. Ivanov and L. V. Keldysh, *Zh. Eksp. Teor. Fiz.* **84**, 404 (1982) [*Sov. Phys.—JETP* **57**, 234 (1983)]). The construction, condition for existence, dispersion, and other properties of the phonoriton are discussed here, based on a simplified model. The relation between creation of phonoritons and inverse Raman scattering is also discussed in this paper. A new nonlinear resonant Brillouin scattering experiment is quantitatively analyzed. For CdS and GaAs the changes in scattering cross section, line shift, and linewidth are calculated: these values should be measurable. A nonlinear modulation-reflection experiment is also analyzed for CdS and GaAs; it gives a measurable change in reflection due to phonoriton reconstruction of the spectrum. We suggest using pulsed irradiation in these experiments. These intensity-dependent effects could directly confirm the existence of phonoritons.

I. INTRODUCTION

The properties of excited states of solids are usually described in terms of various kinds of elementary excitations. The spectra of elementary excitations and the occupation numbers of these quasiparticles determine the physical states of the system. Initially, elementary excitations are well defined only when occupation numbers are small; and so the spectra of various elementary excitations (i.e., various energy levels) are determined by the material itself and are fixed. Actually, these levels also depend on the external perturbations: for example, in optical studies, the probe and pumping electromagnetic radiation. Therefore the spectra can change with increasing occupation number. In nonlinear optics, these changes are manifested through shifts of the energy levels, are often treated by using a phenomenological theory, and are not related to the change of the spectrum. In recent years, the changes of the exciton spectra in bulk and microstructure semiconductors under intense coherent laser pump have attracted great attention because of both theoretical and practical interest.¹⁻⁷ Such phenomena are generally attributed to "dynamical," "optical," or "ac Stark effect," by analogy with similar phenomena in atomic physics, and are also treated by using the methods originating in atomic physics: for example, excitons in semiconductors are only treated as the two-level system, and only the shift of the levels are discussed.

In fact, it is well known that an exciton in a semiconductor is not just an energy level, but also a movable elementary excitation. More importantly, excitons in semiconductors interact with photons all the time and form exciton polaritons. The dispersion relations of the bare exciton and photon are greatly changed near the exciton resonance. This change is not only a renormalization but a drastic change or "reconstruction." A correct theory of the optical spectrum of the exciton must include the exciton effects. And the so-called "optical Stark effect" must

also be established on the basis of the theory of exciton polaritons. Actually, under intense coherent laser pump, the dispersion of the exciton could be reconstructed again, and some new elementary excitations may form. These new "elementary excitations" are different from independent elementary excitations, since their existence and properties depend not only on the intrinsic properties of the material, but also on the external "pump." The "phonoriton" is one such new excitation that will be discussed in this paper.

The term "phonoriton" was coined by Ivanov and Keldysh⁸ in 1982. When a bulk semiconductor with direct gap is illuminated by high-intensity electromagnetic radiation near the exciton resonance, the occupation number for the polariton mode, with frequency equal to that of the incident field, will be very high, and the exciton-phonon interaction, which causes Stokes and anti-Stokes scattering, becomes effectively an intensity-dependent coupling between the scattering polariton modes (final states of Stokes or anti-Stokes scattering) and corresponding phonons. This coupling leads to the formation of a new elementary excitation, the phonoriton, which is a mixture of polariton (photon plus exciton) and phonon. Ivanov, Keldysh, Gippius, and Tikhodeev published a series of papers⁸⁻¹⁵ and analyzed some very interesting aspects of the problem, such as nonlinear light absorption, threshold behavior of anti-Stokes scattering, coherence, etc.

The physics of this problem concerns a many-body system far from thermal equilibrium, and the very dense formalism of the closed-time-path Green's function (CTPGF)¹⁶ was used in most papers by the Keldysh group. But, in fact, in order to understand the essential physical picture and many of the basic properties of the phenomenon, much of the formalism is unnecessary. In this paper we will use a simple two-level model to explain the origin of phonoriton "reconstruction" and discuss its properties. Elsewhere, we will report on certain thresh-

old behavior that we investigated using the CTPGF method.

The previous literature,⁷⁻¹⁵ which gives the basic theory of the phonoriton, is mainly at the level of formal theory and is not well related to realistic physical situations. There has been little experimental response, except for two experimental papers^{17,18} by Soviet scientists claiming that they found indirect evidence of the existence of phonoritons via photoluminescence studies. There are also several other experiments^{4,5} related implicitly to this phenomena, but clear evidence of the phenomena is still not available. Thus, in addition to giving a simple and clear physical picture of the phonoriton, it is also important to design and implement realizable experimental methods to determine the phonoriton and examine its dispersion relations. We have elsewhere proposed two experiments (nonlinear resonant Brillouin scattering (NLRBS) and nonlinear modulation reflection (NLMR) spectrum to determine the properties of the phonoriton, and we gave a brief report of these studies in a short communication.¹⁹ In this paper we will give a detailed description of the theory of the phonoriton and will analyze the NLRBS and nonlinear reflection experiments. We believe these two experiments can give clear evidence of phonoriton reconstruction, and we hope our specific predictions will stimulate further such experiments. We will also discuss the relation of the phonoriton formalism and inverse Raman scattering (IRS).

The organization of the paper is as follows. In Sec. II we will discuss the physical origin of phonoriton reconstruction and give the simplified two-level model. In Sec. III we will discuss the existence condition for the phonoriton and analyze its realization in experiments. In Sec. IV we will discuss the relation between phonoriton formalism and an existing phenomenological macroscopic theory of inverse Raman scattering. Then, Sec. V will be devoted to summarizing the published experiments related to phonoriton, the analysis of our proposed nonlinear resonance Brillouin scattering and nonlinear modulated reflection experiment, and give the results of the calculation for CdS and GaAs. Section VI is a brief summary.

II. TWO-LEVEL-SYSTEM APPROXIMATION

First, let us describe physically how an intense light wave can cause the reconstruction of the spectrum. It is well known that when light with near bandgap frequency enters a semiconductor, the wave propagating inside is not purely electromagnetic but a mixture of photon and exciton, i.e., the exciton polariton. When the frequency is near resonance, the exciton component is rather large, and the polariton will suffer scattering because of the exciton-phonon interaction (e.g., Fröhlich interaction with LO phonon, deformation interaction with LA phonon, and piezoelectric interaction with TA phonon). Since the interaction between exciton and phonon is smaller than that between exciton and photon by several orders of magnitude, usually this only causes Raman or Brillouin scattering. These processes are shown in diagram (a) of Fig. 1. If we consider, as in Fig. 1, the self-energy diagram for a polariton (b) or for a phonon (c), the

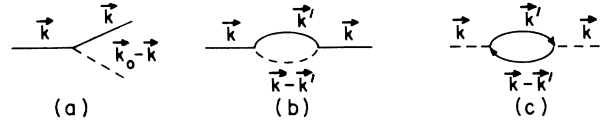


FIG. 1. (a) Polariton-phonon interaction and the self-energy diagram for (b) polariton and (c) phonon.

resulting correction is negligibly small: Only the imaginary part of the self-energy, i.e., the real scattering process, is important. Hence it is usual to consider only the scattering process (a) and not include the rescattering.

On the contrary, when the strength of the incident or pump polariton wave is very large, the mode corresponding to the pump frequency can be macroscopically occupied; thus the ratio N_0/V is finite and not infinitesimally small, where N_0 is the occupation number, and V is the volume. In this case the pumped mode is like a Bose-condensed source, so that anomalous vertex and the Green's function must be included. In the simplest case, the self-energy diagram in Fig. 2 appears. In effect, the result of this diagram is that the macroscopic occupation number of mode k_0 enhances the interaction strength in the vertex in diagrams in Fig. 1. Thus the effect of increasing the incident-light strength is that rescattering processes become important. It is these processes that cause the spectrum reconstruction.

We will not go into details of the exact Green's function theory in this paper, but will only give a two-level approximation.

Following Ivanov and Keldysh,⁸ the Hamiltonian describing the system of interacting photon, exciton, and longitudinal phonon is

$$\begin{aligned}
 H = & \sum_p \hbar \left[\omega_p^{\text{ex}} a_p^\dagger a_p + \omega_p b_p^\dagger b_p + i \frac{\Omega_c}{2} (a_p^\dagger b_p - a_p b_p^\dagger) \right] \\
 & + \sum_p \hbar \Omega_p c_p^\dagger c_p \\
 & + \sum_{i,j,p,q} [iM'_{i,j}(\mathbf{p}-\mathbf{q}) a_p^\dagger a_q (c_{p-q} + c_{-(p-q)}^\dagger) + \text{c.c.}],
 \end{aligned} \tag{1}$$

where $a_p^\dagger, b_p^\dagger, c_p^\dagger$ and a_p, b_p, c_p are creation and annihilation operators for excitons, photons, and phonons, respectively, ω_p is the energy of the photon: $\omega_p = c|\mathbf{p}|/\hbar$, and ω_p^{ex} is the energy of the exciton with momentum \mathbf{p} : $\omega_p^{\text{ex}} = \omega_0 + p^2/2m^*$. Here, ω_0 is the exciton frequency at $p=0$, m^* is the effective mass of exciton, Ω_p is the frequency of the phonon, and $\frac{\Omega_c}{2}$ denotes the photon-exciton interaction, $\Omega_c = \omega_p^{\text{ex}} \sqrt{4\pi\beta}$, where β is the oscillator strength of the exciton, and $M(p-q)$ is the matrix

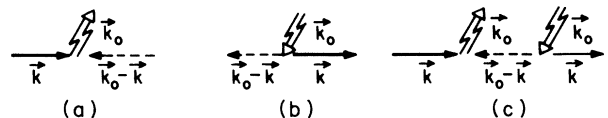


FIG. 2. (a) and (b) Anomalous vertex and (c) self-energy.

element of the exciton-phonon interaction. We can estimate the needed values: For CdS, M is of the order of 10^{-4} cm^{-1} per mode, but Ω_c is 821 cm^{-1} , so that the latter is much stronger. An estimate for GaAs (given below) gives the same conclusion.

The first line of (1) can be diagonalized to give polaritons (two branches), and the whole Hamiltonian can be written as

$$H = \sum_{i,p} \omega_{\text{pol}}(p) B_{i,p}^\dagger B_{i,p} + \sum_p \hbar \Omega_p c_p^\dagger c_p + \sum_{i,j,p,q} [iM'_{i,j}(p-q) B_{i,p}^\dagger B_{j,q} \times (c_{p-q} + c_{-(p-q)}) + \text{c.c.}], \quad (2)$$

where $B_{i,p}^\dagger$ is the creation operator of the i th branch polariton with wave vector \mathbf{p} . The $M'_{i,j}$ are renormalized polariton-phonon matrix elements:

$$M'_{i,j}(p-q) = [\Psi_i^{\text{ex}}(p) \Psi_j^{\text{ex}}(q)]^{1/2} M_{i,j}(p-q). \quad (3)$$

Ψ_i^{ex} is the weight of the exciton in the i th branch polariton:

$$\Psi_{1,2}^{\text{ex}}(p) = \frac{1}{2} \left[1 \mp \frac{\omega_p^{\text{ex}} - \omega_p}{[(\omega_p^{\text{ex}} - \omega_p)^2 + \Omega_c^2]^{1/2}} \right]. \quad (4)$$

Equation (1) contains only a truncated exciton-photon interaction. It is different from the standard Hopfield model,²⁰ which includes additional terms for exciton-photon interaction. The first line of Eq. (1) should then be replaced by

$$\sum_p \hbar \left[\omega_p^{\text{ex}} a_p^\dagger a_p + \omega_p b_p^\dagger b_p + i \frac{\Omega_c \omega_p^{\text{ex}}}{2(\omega_p^{\text{ex}} \omega_p)^{1/2}} \times [(a_p^\dagger b_p - a_p b_p^\dagger) + (a_{-p} b_p - a_{-p}^\dagger b_p^\dagger)] + \pi \beta \omega_p^{\text{ex}} \frac{\omega_p^{\text{ex}}}{\omega_p} (a_p a_p^\dagger + a_p^\dagger a_p + a_p^\dagger a_{-p}^\dagger + a_p^\dagger a_{-p}^\dagger) \right], \quad (5)$$

if we use the Hopfield model. In such a case, this part of Hamiltonian can also be diagonalized to the form shown in Eq. (3), but we should change the dispersion of polariton $\omega_{\text{pol}}(p)$ and the renormalization of the polariton-phonon interaction. The dispersion of the polariton derived from the full Hamiltonian is

$$\frac{ck^2}{\omega^2 \epsilon_b} = 1 + \frac{\Omega_c^2 / \epsilon_b}{(\omega_k^{\text{ex}})^2 - \omega^2}, \quad (6)$$

while that derived from the truncated Hamiltonian can be written as

$$\frac{ck}{\omega(\epsilon_b)^{1/2}} = 1 + \frac{\Omega_c^2 / \epsilon_b}{(\omega_k^{\text{ex}} - \omega)\omega}. \quad (7)$$

Near the resonance, $\omega \approx \omega^{\text{ex}}$, these two equation have only a very small quantitative difference. On the other hand, the renormalized polariton-phonon interaction takes the form

$$M'_{i,j}(\mathbf{p}-\mathbf{q}) = \sqrt{A_i(\mathbf{p}) A_j(\mathbf{q})} \times \left[\frac{1}{2} + \frac{\omega_p^{\text{pol}} \omega_q^{\text{pol}}}{\omega_p^{\text{ex}} \omega_q^{\text{ex}}} \right] M_{i,j}(\mathbf{p}-\mathbf{q}). \quad (8)$$

Here,

$$A_i(p) = \frac{\Omega_c^2 \omega_i(p) \omega_{\text{ex}}(p)}{[\omega_i^2(p) - \omega_{\text{ex}}^2(p)]^2} \left[\epsilon_b + \frac{\Omega_c^2 \omega_{\text{ex}}^2(p)}{[\omega_i^2(p) - \omega_{\text{ex}}^2(p)]^2} \right] \quad (9)$$

is the so-called exciton strength function $A_i(p)$ and corresponds to the exciton weight factor Ψ_i^{ex} in the truncated Hamiltonian. Because both $A_i(p)$ and Ψ_i^{ex} are near unity, we will use the simple truncated Hamiltonian to explain the phonoriton reconstruction. For the numerical calculations in Sec. V we will use the results from the standard Hopfield model.

Now, suppose a beam of light with frequency ω_0 enters the system and creates a polariton wave. For the sake of simplicity, we restrict ourselves to one branch of polariton corresponding to the frequency ω_0 and denote this branch by l . We denote this wave as $\omega_0 = \omega_{\text{pol}}(\mathbf{k}_0)$, where $\omega_{\text{pol}}(\mathbf{k})$ is the dispersion of the polariton. When the intensity of the beam is high, the polariton mode $\mathbf{k} = \mathbf{k}_0$ will be ‘‘macroscopically occupied.’’ But for all other modes, the occupation number is near zero. Thus the interaction terms related to mode k_0 should be treated separately. On the other hand since, the polariton-phonon interaction not related to the mode k_0 is rather weak; this merely contributes to a nonzero imaginary part of the polariton energy. Therefore, we drop these terms. Then we divide the system into three parts: incident polariton, phonon, and scattered polariton. We concentrate on the scattered polaritons and phonons. They are coupled by the polariton-phonon interaction $MB_{k_0}^\dagger$ and MB_{k_0} . If the incident laser light is coherent and the intensity high enough, to a good approximation we can replace the operators $B_{k_0}^\dagger$ or B_{k_0} in the interaction term by their c -number expectation values $\langle B_{k_0}^\dagger \rangle$ and $\langle B_{k_0} \rangle$, respectively:

$$\alpha^*(t) = \left[\frac{\epsilon_b V}{2\pi v_g \beta} \right]^{1/2} P_0 e^{-i\omega_{k_0} t} = \alpha_{k_0} e^{-i\omega_{k_0} t}, \quad (10)$$

or

$$\alpha(t) = \left[\frac{\epsilon_b V}{2\pi v_g \beta} \right]^{1/2} P_0 e^{i\omega_{k_0} t} = \alpha_{k_0} e^{i\omega_{k_0} t}, \quad (10')$$

with

$$\alpha_{k_0} = \left[\frac{\epsilon_b V}{2\pi v_g \beta} \right]^{1/2}, \quad (11)$$

where v_g is the group velocity of the polariton, P_0 is the macroscopic polarization amplitude, and ϵ_b is the dielectric constant of the background. Actually, these two numbers $\alpha^*(t)$ and $\alpha(t)$ come from the ‘‘eigenvalues’’ of the annihilation operator B_{k_0} acting on a coherent state of the polariton mode \mathbf{k}_0 , which occurs because of the

high intensity of pumping. After eliminating the time-dependent factor $e^{-i\omega_{k_0}t}$ via a unitary transformation $e^{i\omega_{k_0}B_k^\dagger B_k t}$, we obtain the Hamiltonian:

$$H_{k_0} = \sum_{p,i} \hbar(\omega_{p,i} - \omega_{k_0}) B_{p,i}^\dagger B_{p,i} + \sum_{\mathbf{p}} \hbar \Omega_{\mathbf{p}} c_{\mathbf{p}}^\dagger c_{\mathbf{p}} + H_S + H_{AS}, \quad (12)$$

where

$$H_{AS} = i \sum_{\mathbf{p}} \hbar M'(\mathbf{p}-\mathbf{k}) \alpha_{k_0} (B_{\mathbf{p}}^\dagger c_{\mathbf{p}-\mathbf{k}_0} - B_{\mathbf{p}} c_{\mathbf{p}-\mathbf{k}_0}), \quad (13)$$

and

$$H_S = i \sum_{\mathbf{p}} i \hbar M'(\mathbf{p}-\mathbf{k}) \alpha_{k_0} (B_{\mathbf{p}} c_{\mathbf{k}_0-\mathbf{p}} - B_{\mathbf{p}}^\dagger c_{\mathbf{k}_0-\mathbf{p}}) \quad (14)$$

are anti-Stokes and Stokes scattering Hamiltonians, respectively. Here

$$M'_{i,j}(p-q) = [\Psi_i^{\text{ex}}(p) \Psi_j^{\text{ex}}(q)]^{1/2} M_{i,j}(p-q) \quad (15)$$

is the matrix element between polariton and phonon, and Ψ_i^{ex} is the weight of the exciton in the i th branch polariton.

Since the ‘‘interaction’’ between the spectra at anti-Stokes and Stokes frequencies is essentially a high-order effect, we may study the spectra around anti-Stokes and Stokes frequencies individually. If we only consider H_{AS} , we are, in effect, describing a simple two-level system. The scattered-polariton mode ($\omega_{p,i} - \omega_{k_0}$), i.e., the energy with respect to incident light, and phonon $\Omega_{\text{ph}}(\mathbf{p}-\mathbf{k}_0)$ are coupled through the interaction $\sqrt{N_0} M'_{i,j}(\mathbf{p}-\mathbf{k}_0)$, and this interaction is proportional to the square root of the strength of the incident macroscopically filled polariton mode. From now on, we will concentrate on a specific branch and drop the subscript i or ij of B and M . If we introduce a linear combination of the annihilation operators of the polariton and phonon,

$$D = vB_p + uc_{\mathbf{p}-\mathbf{k}_0}, \quad (16)$$

and demand that

$$[D, H] = -\hbar\omega D, \quad (17)$$

we find the secular equation, giving eigenvalues

$$\omega_{1,2}(\mathbf{p}) = \frac{1}{2} [\omega(\mathbf{p}) + \Omega_{\mathbf{k}_0-\mathbf{p}} - \omega_{k_0}] \pm \frac{1}{2} \{ [\omega(\mathbf{p}) - \Omega_{\mathbf{p}-\mathbf{k}_0} - \omega_{k_0}]^2 + \Psi_{\text{ex}}(\mathbf{p}) Q^2 \}^{1/2}, \quad (18)$$

$$Q = \alpha_k M(\mathbf{p}-\mathbf{k}) = (\sqrt{N_0})^{1/2} M(\mathbf{p}-\mathbf{k}), \quad (19)$$

where N_0 is the occupation number of the incident polariton. Note that near the exciton resonance $\Psi_i^{\text{ex}}(\mathbf{k})$ there is practically unity. Equation (19) gives the reconstructed spectrum of the new excitation, or phonoriton: see the illustration in Fig. 3(c). A new gap, $\{ [\omega(p) - \Omega_{\mathbf{p}-\mathbf{k}_0} + \omega_{k_0}]^2 + \Psi_{\text{ex}}(p) Q^2 \}^{1/2}$ appears, generalizing the gap $\omega_{\text{LO}} - \omega_{\text{TO}}$ of the polariton. The new gap not only depends on the properties of the material, but is

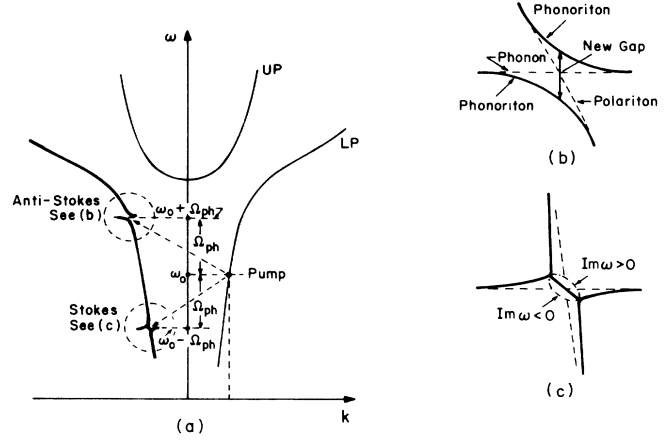


FIG. 3. The dispersion of the anti-Stokes phonoriton related to LO phonon. The pump frequency is at ω_0 , and the optical phonon Ω_{ph} is assumed dispersionless: (a) General illustration; (b) detailed behavior at anti-Stokes frequency; (c) detailed behavior at Stokes frequency.

also proportional to the square root of the intensity of the pump light. This is a salient feature of the phenomena.

For the case of Stokes scattering, we can introduce

$$D = xB_p + yc_{\mathbf{k}_0-\mathbf{p}}.$$

The basic equation is the same as for the anti-Stokes scattering case, but with some changes of the signs.

We can also include lifetime effects and combine the resulting expressions for both Stokes and anti-Stokes scattered phonoritons as follows:

$$\omega_{1,2}^\pm(\mathbf{p}) = \frac{1}{2} [\omega(\mathbf{p}) \pm \Omega_{\mathbf{k}_0-\mathbf{p}} - \omega_{k_0} + i\Gamma] + (-) \frac{1}{2} \{ [\omega(\mathbf{p}) \mp \Omega_{\mathbf{k}_0-\mathbf{p}} + \omega_{k_0} + i\gamma]^2 \pm \Psi_{\text{ex}}(\mathbf{p}) Q^2 \}^{1/2}, \quad (20)$$

with

$$\Gamma = \gamma_{\text{ph}} + \gamma_{\text{pol}}, \quad (21)$$

and

$$\gamma = \gamma_{\text{ph}} - \gamma_{\text{pol}}, \quad (22)$$

where γ_{ph} and γ_{pol} are the inverse lifetimes of phonon and polariton, respectively. The \pm sign in Eq. (20) is for Stokes (+) and anti-Stokes (-) scattering, while $+(-)$ is for the two branches in each case. This expression for phonoriton dispersion given by the two-level model is equivalent to the τ approximation in CTPGF theory¹² of Keldysh and Tikhodeev.

Figure 3 illustrates the dispersion of the phonoriton described by Eq. (20). Note that we consider only the optical phonon scattering and only in the back-scattering geometry; the reason for this will be explained in Sec. III. The drawing is only schematic and assumes that γ_{ph} and γ_{pol} are both zero. Note that there are two important changes in the dispersion of the parent polariton in back scattering. First, a new gap appears in the dispersion at

the location of the anti-Stokes scattered polariton. Second, there is no real gap, but an "imaginary" gap appears in the case of Stokes scattering.

The latter should be given special attention. Note that the sign before the "interaction" term under the square root is negative. Thus it would not give rise to repulsion and anticrossing of two original levels and create a new gap. On the contrary, two levels will attract each other and give rise to an "imaginary gap." In fact, both γ_{ph} and γ_{pol} are not zero; therefore under certain conditions, the imaginary part of the energy of one branch of the phonoriton will change its sign, and this will invalidate the approximation here. The situation corresponds to stimulated Stokes scattering. In the remaining part of this paper, we will concentrate on anti-Stokes scattering and the new gap. The threshold problem for stimulated scattering will be discussed elsewhere.

Now let us explain the physical origin of the new coupling caused by the pump light. What we should note is that the spectrum under consideration is not the spectrum of the original crystal itself, but a new system: the crystal with the strong pump polariton (\mathbf{k}_0, ω_0) propagating in it. The presence of this wave makes any polariton with wave vector k interact with a phonon with wave vector $k \pm k_0$ and frequency $\omega(k) \pm \omega_0$. The nonlinear phonon-polariton interaction in the "old system" (crystal only) becomes an effective linear coupling between polariton and phonon. In the new system (crystal plus existing strong waves), it plays the role of new periodic "potential" or diffraction "grating," with spatial periodicity $2\pi/k_0$ for polaritons and phonons that satisfy the scattering conditions. Of course, this potential is different from the ordinary potential, because it acts between two different elementary excitations, it is also dynamical not static, and it depends on the external laser field. It is this "Bragg-like" diffraction that couples the polariton and phonon that satisfy the "scattering" condition and thus produces the spectrum reconstruction.

III. PHONORITON EXISTENCE CONDITIONS: CALCULATION FOR CdS AND GaAs

A. General consideration

The conditions for existence of a phonoriton were discussed in previous work on the phonoriton⁸ and then clarified later by Ivanov.¹⁰ In this section we will discuss the physical meaning of these conditions and then give some concrete estimations for CdS and GaAs.

From the discussion in Secs. II and III, it is clear that, in order to form a phonoriton, we first should have a polariton wave propagating inside the substance, and this wave should propagate a sufficient distance to be able to interact with phonons. Therefore, we need

$$\text{Re}(\mathbf{k}) \gg \text{Im}(\mathbf{k}) , \quad (23)$$

From the dispersion [Eq. (7)], this condition can be satisfied if the frequency ω_0 is in the range of

$$|\omega_t - \omega_0| \gg (\frac{1}{4}\omega_t^2 + \gamma\omega_t)^{1/2} - \frac{1}{2}\omega_{lt} ,$$

where ω_{lt} is the difference between longitudinal and transverse bare excitons, and γ is the inverse lifetime of the polariton. Although this condition arose from the truncated Hamiltonian, it should not be greatly different from that obtained from the full Hamiltonian.

Second, in order to interact with phonons, this wave should be excitonlike, i.e., the exciton weight factor $\Psi^{\text{ex}}(k_0)$ should near 1. According to (4),

$$|\omega_t - \omega_0| \leq \Omega_c .$$

Because a high occupation number should be achieved, at given linewidth of the source and scattering mechanism, the density of states near the frequency ω_0 should be low. Thus the pump light should be in the lower polariton branch, and the combined requirement can be written as

$$\Omega_c \geq \omega_t - \omega_0 \gg (\frac{1}{4}\omega_{lt}^2 + \gamma\omega_t)^{1/2} - \frac{1}{2}\omega_{lt} . \quad (24)$$

Needless to say, only photon-exciton interaction in direct-gap semiconductors is considered here.

It is clear from Eq. (19) that, when the intensity of the pump light increases from zero, the change of the spectrum also increases. But if the real part of the splitting is smaller than the imaginary part, the splitting and the spectrum reconstruction cannot manifest themselves. This condition can be expressed as

$$\Delta\omega > \gamma_{\text{pol}} + \gamma_{\text{ph}} . \quad (25)$$

$\Delta\omega$ could be obtained from Eq. (16). Physically, we can understand this as following: If the lifetime of the phonon and polariton is shorter than the inverse of the scattering and rescattering rate, then the scattered polariton and phonon cannot be correlated coherently; thus the only physical consequence is the real scattering process, not the spectrum anticrossing.

Ivanov has summarized the conditions for phonoriton existence as the following:¹⁰

$$\Omega_c > \Omega(p - k_0) , \quad (26a)$$

$$[2\Delta(p - k_0)\Omega(p - k_0)]^{1/2} \geq \gamma(p) + \gamma_{\text{ph}}(p - k_0) , \quad (26b)$$

$$\Delta(p - k_0) > \gamma_{\text{pol}}(k) . \quad (26c)$$

Actually, (26a) is satisfied by most direct-gap semiconductors; but even for the direct-gap materials, in which (26a) is not valid, Ω_c still is of the same order of magnitude as $\Omega(p - k_0)$. As for (26b) and (26c), when (25) is valid, they are also satisfied automatically.

Now we discuss the strength of different kinds of phonon-polariton interactions and give some numerical estimates to determine which of these channels could be the most probable candidate for phonoriton reconstruction. For more details of these interactions, see, e.g., Ref. 21.

The matrix elements we will discuss below are restricted to the case when only two 1s excitons are involved, i.e.,

$$M(\mathbf{q}) = \langle \mathbf{k} - \mathbf{q}, 1s, n_q + 1 | H_{\text{ex-ph}} | n_q, 1s, \mathbf{k} \rangle . \quad (27)$$

The exciton can interact with longitudinal acoustic

phonons through the deformation-potential interaction. In this case,

$$M(\mathbf{q}) = \left[\frac{\hbar}{2V\rho c_{\text{LA}}} \right]^{1/2} |\mathbf{q}|^{1/2} (p_e D_e + p_h D_h), \quad (28)$$

where V is the volume of the crystal, ρ is the density of the material, c_{LA} is the velocity of the longitudinal acoustic wave, D_e and D_h are the deformation potential of electron and hole, respectively; p_e and p_h are two factors defined as the following:

$$p_e = \left[1 + \frac{m_h^*}{m_h^* + m_e^*} \left(\frac{qa_B}{2} \right)^2 \right]^{-2}, \quad (29)$$

$$p_h = \left[1 + \frac{m_e^*}{m_h^* + m_e^*} \left(\frac{qa_B}{2} \right)^2 \right]^{-2}. \quad (30)$$

Here, m_e^* and m_h^* are the effective masses of electron and hole, respectively. a_B is the Bohr radius of the 1s exciton. These two factors can be called form factors. They describe the effect of the distribution of the electron and hole in the exciton on the interaction of the exciton as a whole in a field with wave vector \mathbf{q} . If the wave vector of phonon q is zero, or if the electron and hole are in the same place ($a_B=0$), they become unity. If $qa_B = \infty$, they become zero. In our case, $qa_B < 1$, even $\ll 1$, so that the factor $(p_e - p_h)$ can be expanded to obtain the following expression:

$$(p_e - p_h) \xrightarrow{qa_B \ll 1} \frac{m_h^* - m_e^*}{m_h^* + m_e^*} \frac{(qa_B)^2}{2}. \quad (31)$$

The matrix elements of the Fröhlich interaction between two 1s exciton states can be expressed as

$$M(\mathbf{q}) = \left[\frac{2\pi\hbar\omega_0 e^2}{Vq^2} \right]^{1/2} \left[\frac{1}{\epsilon_\infty} - \frac{1}{\epsilon_0} \right]^{1/2} (p_e - p_h), \quad (32)$$

where ω_0 is the frequency of the LO phonon, e is the charge of the electron, and ϵ_∞ and ϵ_0 are the high-frequency and static dielectric constants, respectively.

An optical phonon can also interact with the exciton through optical deformation interaction and is additive to the polar interaction; but, since it is generally much weaker than polar (Fröhlich) interaction, we can neglect it here.

There is another interaction in noncentrosymmetric materials, namely, the piezoelectric interaction, coupling the exciton with TA phonons. In contrast to the deformation and polar interaction, which are isotropic in cubic crystals, the piezoelectric interaction is highly anisotropic, even in cubic materials. For GaAs, when the phonon wave vector \mathbf{q} is along [110] direction the matrix element is

$$M(\mathbf{q}) = \left[\frac{\hbar}{q\rho c_{\text{TA}}} \right]^{1/2} \frac{4\pi e e_{15}}{\epsilon_0 q^{1/2}} (p_e - p_h), \quad (33)$$

where e_{15} is the piezoelectric constant, c_{TA} is the velocity of the TA acoustic waves, ϵ_b is the dielectric constant of the background.

For CdS, when wave vector \mathbf{q} is along the z axis, e_{15} should be replaced by e_{14} .

Therefore, in all three cases, the interaction increases when the transfer of momentum $|\mathbf{q}|$ increases, in the range of $qa_B < 1$. Thus the greatest splitting will occur in the back-scattering geometry.

B. Numerical estimations for CdS and GaAs

Let us take CdS and GaAs as examples to estimate the value VM^2 for different scattering mechanisms. The parameters and calculated results are shown in Table I.

This calculation indicates that the Fröhlich interaction is much stronger than other interactions. Thus we focus our attention on the phonon constructed from exciton-polariton and LO phonon. Even in this case, the power density needed to produce a noticeable gap is still very high.

For example, in order to detect the appearance of the gap, the splitting should be greater than 10^{-4} eV, and N_0 should be at least $10^{16-17} \text{ cm}^{-3}$. The power density is $S = N_0 v_g \hbar \omega$, where v_g is the group velocity of the polariton. The value of v_g could vary greatly near the crossing or near the bottleneck for the polariton. Of course, the value of S can also be small, if the frequency is above the bottleneck. But in this case, the nearby density of states is large and the scattering lifetime is also reduced, which could lead to more absorption, severe heating effects, and also line broadening. Thus a most probable choice of pump frequency is below the bottleneck, and this also simplifies the analysis.

If we choose the pump energy below the bottleneck by approximately a LO phonon energy, the complexity caused by exciton-biexciton transition under high-intensity excitation will be greatly alleviated, since the binding energy of the biexciton, $2\omega_{\text{ex}} - \Omega_{\text{biex}}$, is much smaller than ω_{LO} , and the change of the spectrum caused by exciton-biexciton transition is also much smaller than ω_{LO} .^{6,7}

Thus we can choose a pump frequency, at $\omega_T - \omega_{\text{LO}}$. In this case, the estimated power density for GaAs is 10^7 W/cm, and for CdS, $\sim 10^8$ w/cm.

It should be noted also that although CdS is more polar than GaAs, the power needed for generating the same gap is smaller in GaAs. This is because the Bohr radius of the exciton in GaAs is much larger than that in CdS, because the overall interaction is proportional to the fourth power of a_B , and also because the difference between the effective masses of electrons and holes in GaAs is bigger. But the exciton-photon coupling Ω_c (or the L - T splitting of exciton) in GaAs is small, thus the polariton can only manifest itself in a narrow range, and the exciton strength function is very small outside this range. On the other hand, for CdS, the exciton radius a_B is smaller, which makes the exciton-phonon interaction weaker; however, the Ω_c is bigger, and in wider frequency range, the polariton effect is strong, and the scattering, via larger wave-vector transfer \mathbf{q} , can also be achieved. So both materials could be chosen for the experiment to detect phononitons.

In any case, the phononiton reconstruction is a

TABLE I. The parameters and calculated results for CdS and GaAs. Asterisk denotes Ref. 22. All other data for CdS are adopted from Ref. 23. For GaAs, Ref. 24. Double asterisk denotes e_{15} . Triple asterisk denotes $E_c - E_v$.

		CdS	GaAs
Exciton energy	E_t , eV	2.553	1.515
L - T splitting	E_{lt} , meV	1.9	0.08
Effective mass of electrons	m_e^* , m_0	0.198	0.0667
Effective mass of hole	m_h^* , m_0		0.138 (lh)
Effective mass of exciton	M_{ex}^* , m_0	0.98	0.6±0.1
Background dielectric constant	ϵ_b	9.38	12.55
Bohr radius of exciton	a_B , Å	28	138
Conduction-band deformation potential	E_c , eV	+4.5	9.2 ***
Valence-band deformation potential	E_v , eV	-2.9	
Density	ρ , g/cm ³	4.84	5.36
Velocity of the longitudinal acoustic wave	C_{LA} , 10 ⁵ cm/sec	4.25	5.24
Velocity of the transverse acoustic wave	C_{TA} , 10 ⁵ cm/sec	1.76	3.36
Piezoelectric constant	e_{14} , C/m ²	-0.21	0.16**
Static dielectric constant	ϵ_0	9.53*	12.90*
High-frequency dielectric constant	ω_∞	5.61*	10.90*
Frequency of LO phonon at Γ	ω_{LO} , eV	38*	36.9*
Wave number of phonon used in calculation	q , 10 ⁵ cm ⁻¹	7.9	5.4
Form factor of electron	P_e	0.998788	0.8084
Form factor of hole	P_h	0.985266	0.9853
	$(P_e - P_h)^2$	1.828×10^{-4}	3.65×10^{-2}
Matrix elements of exciton-LA phonon interaction	$ M' ^2$, eV ² cm ⁻⁴	5.12×10^{-28}	9.32×10^{-27}
Matrix elements of exciton-TA phonon interaction	$ M' ^2$, eV ² cm ⁻⁴	9.15×10^{-29}	5.47×10^{-29}
Matrix elements of exciton-LO phonon interaction	$ M' ^2$, eV ² cm ⁻⁴	7.34×10^{-25}	5.83×10^{-23}
Exciton strength function at $E_T - \omega_{LO}$	A_i	0.64	0.044
Matrix elements of polariton-LO phonon interaction	$ M' ^2$, eV ² cm ⁻⁴	4.69×10^{-25}	2.57×10^{-24}

phenomenon occurring only under very strong irradiation. Thus, in our view, the possible realizations of the related experiment should be under pulse condition. Thus we need to know the lifetime of phonoriton. From Eq. (16), we can also obtain a simple relation:

$$\text{Im}\omega_1 + \text{Im}\omega_2 = \gamma_{ph} + \gamma_{pol}. \quad (34)$$

In the case of anti-Stokes scattering, if the splitting (the real part of $\Delta\omega$) is much larger than the linewidth, the lifetime of the phonoriton is of the same order of magnitude as that of the polariton and related phonon.

We can also examine the incident mode and others nearby. They are also coupled via the phonons, and the "coupling constant" is proportional to the density of scattered polariton modes. Therefore, these polariton modes are also changed, although the change is not as prominent as for the scattered polaritons. If we treat the problem more exactly, the initial polariton, scattered polariton, and related phonon are all coupled to form the phonoriton. Actually, the scattering, rescattering, and spectrum reconstruction results in nonlinear absorption of the pump light.⁸

It should be noted that the discussion above uses a rather strong approximation—replacing the operators of the pump mode by c numbers. This is true only when the polariton wave is coherent, and, of course, the treatment is similar to the classical one. The limitation of this approximation is that it cannot be used to treat some quantum aspects of the problem, such as coherence, noise, and dynamical behavior, which will be discussed elsewhere.

On the other hand, this model gives the basic physical picture in the problem and enables us to relate the topic to some existing phenomenological theories of nonlinear phenomena.

IV. PHONORITON: RELATION TO INVERSE RAMAN SCATTERING

The physical situation of phonoriton reconstruction via a LA or TA phonon is very similar to the case of resonant Brillouin scattering (RBS) of an exciton polariton proposed by Brenig, Zeyher, and Birman,²⁵ except that the intensity of the pump light is high, and we focus on the spectrum around the scattered frequency. For the most probable case of reconstruction with the LO phonon, it corresponds to resonant Raman scattering. In the traditional theory of the Raman and Brillouin scattering, the energy levels are fixed. Even in the case of intense excitation, work focused on stimulated Raman and Brillouin scattering, and not on the change of the energy levels, due to the fact that the change of the spectrum is very small. However, if the spectrum were measured, the change of the energy levels still can be detected. This is the case of the variation of dielectric function in inverse Raman spectroscopy (IRS).

IRS was first proposed and experimentally confirmed by Jones and Stoicheff.²⁶ They pointed out that according to the basic theory of incoherent light scattering, the emission and absorption of light at Stokes and anti-Stokes frequencies are both allowed. Actually, this is the consequence of the time-reversal invariance of the interaction

Hamiltonian. Thus, not only stimulated emission, but also “stimulated” absorption should be possible. Pump light can induce absorption at the Stokes and anti-Stokes mode and change the dielectric function, which forms the basis of IRS. In this sense, IRS is really the inverse process of stimulated Raman scattering, (SRS) so that the absorption line shape should be the inverse of that of the gain profile in SRS measurement. But the experiments afterwards gave more complex absorption line shapes, and this has to be explained theoretically. In 1985, Saikan *et al.*²⁷ developed a theory of IRS. They analyzed the dependence of the third-order nonlinear susceptibility on the initial values of the density matrix and pointed out that the line shape of IRS is not exactly the inverse of the gain spectrum of SRS because of this. More important, they obtained an expression more general than that obtained using third-order perturbation theory for the nonlinear susceptibility. Recall that the definition of the third-order nonlinear polarizability χ_{nl} , under irradiation by a strong pump light beam, with frequency ω and amplitude E . The polarization $P(\omega')$, induced by a probe field E' at frequency ω' , is

$$P(\omega') = \chi^{(1)}(\omega')E' + \chi^{(3)}(\omega', \omega)E'|E|^2. \quad (35)$$

More generally, we can take this as a Taylor expansion of a general polarizability $\chi(\omega', E)$, so that

$$\begin{aligned} \chi(\omega') &= \frac{|\mu_{bc}|^2}{h} \frac{\omega_{ab} - \omega' + \omega - i\gamma_{ac}}{(\omega_{ac} - \omega' + \omega - i\gamma_{ac})(\omega_{ab} - \omega' - i\gamma_{ac}) - |\mu_{ab\omega}/h|^2} \\ &= \frac{|\mu_{bc}|^2}{h} \left[\frac{\frac{1}{2}[1 - \delta/(\delta^2 + \beta^2)^{1/2}]}{\omega_{bc} - \delta - (\delta^2 + \beta^2)^{1/2} + \omega' - i\Gamma_{bc}} + \frac{\frac{1}{2}[1 + \delta/(\delta^2 + \beta^2)^{1/2}]}{\omega_{bc} - \delta + (\delta^2 + \beta^2)^{1/2} + \omega' - i\Gamma_{bc}} \right], \end{aligned} \quad (37)$$

where

$$\delta = \frac{1}{2}[\omega_{ba}^0 - \omega + i(\gamma_{ac} - \Gamma_{bc})], \quad (38)$$

$$\beta^2 = |\mu_{ab}E(\omega)/h|^2. \quad (39)$$

The results can be understood as the following: Under the interaction of $Ee^{\pm i g \omega t}$, the energy level E_b shifts and splits into two, as shown in Fig. 4(b), and the weights of the oscillator strength of the two components are $\frac{1}{2}[1 - \delta/(\delta^2 + \beta^2)^{1/2}]$ and $\frac{1}{2}[1 + \delta/(\delta^2 + \beta^2)^{1/2}]$. Obviously, this is a kind of *dynamical* Stark effect, because the perturbation field is time dependent. If we take the detuning $\omega_{ba}^0 - \omega$ equal to zero, i.e., at resonance, and compare the denominators with the reconstructed spectrum of the phonoriton [Eq. (16)], the structure is the same.

However, the “reconstruction” in the denominator does not exactly correspond to the phonoriton. First, it is related to an electronic process through the perturbation on the occupation numbers of the levels, while the phonoriton reconstruction depends on electron-phonon interaction enhanced by strong pump waves. Second, despite formal resemblance, the reconstruction in the denominator only corresponds to the coupling between exciton and phonon, which does not include the polariton effects.

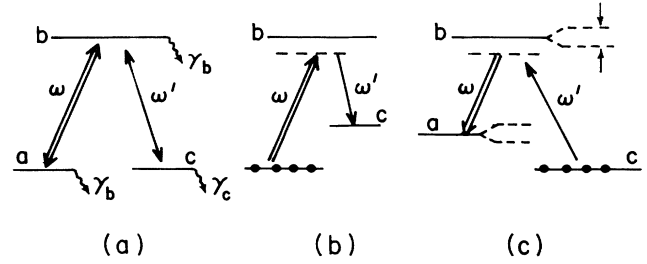


FIG. 4. (a) Three-level configuration, (b) the stimulated Raman gain spectroscopy, and (c) the inverse Raman spectroscopy.

$$P(\omega') = \chi(\omega', \omega, E)E'. \quad (36)$$

By using the so-called ladder approximation,²⁸ they obtained the expression for such a susceptibility for a three-level model, which is illustrated schematically in Fig. 4. The transition frequency between the levels are denoted as $\omega_{ac}, \omega_{ab}, \omega_{bc}$, and the corresponding transition matrix elements and linewidth as μ 's and γ 's. Under intense irradiation of light of frequency ω near the resonance with the transition ω_{ab} , the polarizability at ω' near the transition ω_{bc} can be written as

It should be emphasized that it is not the IRS effect which itself corresponds to the phonoriton reconstruction, but the change of the energy spectrum induced by a strong dynamical perturbation can be manifested in the IRS experiment. The most important difference is the following. In the theory of the dielectric function used in IRS, only the change of dielectric function was considered, and this is due to the nonlinear susceptibility. The changes of the spectrum of the phonon and the (scattered) polariton were not included; in other words, the perturbation or probe field is assumed to exist. Contrary to this, the phonoriton reconstruction emphasizes the change of the spectrum, and the mixed mode of phonon and polariton becomes an intrinsic property of the system under intense excitation whether or not the probe field is present. This new renormalized elementary excitation could be detected by any probe that can interact with it (e.g., the RBS experiment that we will discuss later in this paper), while the IRS theory could not predict such an effect. Besides, since the phonoriton theory starts from a microscopic level, it can give the microscopic origin and can be used to study the quantum aspects of the problem, such as coherence and noise. Therefore, although the phonoriton has some apparent similarity to the entity already studied in IRS, it is actually different in content.

In order to clarify the phonoriton-IRS relationship still further, let us write down the macroscopic equations for the electric field \mathbf{E} , exciton polarization amplitude \mathbf{P} , and phonon amplitude \mathbf{U} . One gets

$$\frac{\epsilon_g}{c^2} \frac{\partial^2}{\partial t^2} \mathbf{E} - \frac{\partial^2}{\partial z^2} \mathbf{E} = \frac{4\pi}{c} \frac{\partial^2}{\partial t^2} \mathbf{P}, \quad (40)$$

$$\begin{aligned} \frac{\partial^2}{\partial t^2} \mathbf{P} - \left[\omega_0^2 + \frac{\hbar\omega_0}{m^*} \frac{\partial^2}{\partial z^2} \right] \mathbf{P} \\ = \frac{4\pi}{c} \frac{\delta}{\delta \mathbf{P}} \int \mathcal{D} : \mathbf{U} \mathbf{P} \mathbf{P} \, dr + \alpha \mathbf{E}, \quad (41) \end{aligned}$$

$$\frac{\partial^2}{\partial t^2} \mathbf{U} - \omega_{\text{ph}}^2 \mathbf{U} = \frac{\delta}{\delta \mathbf{U}} \int \mathcal{D} : \mathbf{U} \mathbf{P} \mathbf{P} \, dr. \quad (42)$$

For simplicity, the phonon is assumed to be dispersionless. Note that \mathcal{D} is a third-order tensor and depends on the frequencies and wave vectors of three different waves \mathbf{U} , \mathbf{P} , and \mathbf{P} . When the frequency and wave vector satisfy

the conservation condition, its value becomes large, and this nonlinear term cannot be neglected.

Equations (40)–(42) are difficult to solve because of the presence of nonlinear terms. In our case, we can first make an approximation that the component of exciton polarization amplitude \mathbf{P} at frequency ω_0 if incident light has already been obtained,

$$P_{\omega_0} = P_0 e^{i(\omega_0 t - \mathbf{k}_0 \cdot \mathbf{r})}, \quad (43)$$

and then concentrate on the components of electric field \mathbf{E} and \mathbf{P} around the Stokes ω_S and anti-Stokes frequency ω_{AS} , and the lattice vibration \mathbf{U} . We search for the solutions of the form $e^{i(\omega t - \mathbf{k} \cdot \mathbf{r})}$. Remember that we should only include the nonlinear term between the intense component of polarization $\mathbf{P}_{\omega_0} = P_0 e^{i(\omega_0 t - \mathbf{k}_0 \cdot \mathbf{r})}$ and polarization $\mathbf{P}(\mathbf{k}, \omega)$, and vibration $\mathbf{U}(\mathbf{k} - \mathbf{k}_0, \omega - \omega_0)$ (anti-Stokes case) or $\mathbf{U}(\mathbf{k} - \mathbf{k}_0, \omega_0 - \omega)$ (Stokes case). We can get the eigenvalue equation,

$$\left[\omega^2 - \frac{c^2 |\mathbf{k}|^2}{\epsilon_b} \right] \left[\omega^2 - \omega_{\text{ex}}^2(\mathbf{k}) \right] \left[(\omega - \omega_0)^2 - \omega_{\text{ph}}^2(\mathbf{k} - \mathbf{k}_0) \right] - \frac{4\pi\alpha\omega^2}{c} \left[(\omega - \omega_0)^2 - \omega_{\text{ph}}^2(\mathbf{k} - \mathbf{k}_0) \right] - \left[\omega^2 - \frac{c^2 |\mathbf{k}|^2}{\epsilon_b} \right] |\mathcal{D}\mathbf{P}_0|^2 = 0, \quad (44)$$

and the dielectric function,

$$\epsilon(\omega, \mathbf{k}) = \epsilon_b + \frac{4\pi\alpha\omega^2}{[\omega^2 - \omega_{\text{ex}}^2(\mathbf{k})] + [|\mathcal{D}\mathbf{P}_0|^2 / (\omega - \omega_0)^2 - \omega_{\text{ph}}^2(\mathbf{k} - \mathbf{k}_0)]}. \quad (45)$$

If we equate $\epsilon(\omega, \mathbf{k})$ to $c^2 k^2 / \omega^2$, then this eighth-order equation for ω could give, at most, eight solutions for a given \mathbf{k} , corresponding to the positive and negative frequency of the four branches of the phonoriton from two parent branches of the polariton.

Here \mathcal{D} is a phenomenological parameter, it depends on the frequency, and it should be obtained from microscopic theory. Thus we prefer to get the dielectric function from the microscopic picture directly. If we start with the standard Hopfield Hamiltonian for polariton and add exciton-phonon Hamiltonian, once we take the operators of the macroscopic occupied mode as a c number, the calculation of dielectric function is routine (see, e.g., Mahan²⁹). The result is

$$\epsilon(\omega, \mathbf{k}) = \epsilon_b + \frac{4\pi\alpha\omega^2}{[\omega^2 - \omega_{\text{ex}}^2(\mathbf{k}) + \{ [N_0 |M(\mathbf{k} - \mathbf{k}_0)|^2]^2 / (\omega - \omega_0)^2 - \omega_{\text{ph}}^2(\mathbf{k} - \mathbf{k}_0) \}]}. \quad (46)$$

It should be remembered here that ω_0 is the frequency of the intense pump mode and the \mathbf{k}_0 polariton, and N_0 is the occupation number of this mode.

The most prominent feature of the new dielectric function is its dependence on the external perturbation field, and, in particular, it has additional poles, the position of which depends on the perturbation. This gives the possibility of controlling the light by light.

Of course, one can use a simple truncated Hamiltonian and only take the positive frequency, obtaining the results similar to (37). However, the difference between (37) and (46) is very small and, in practice, of no significant importance.

V. EXPERIMENTAL DETECTION OF THE PHONORITON

In this section we will discuss several published experiments related to the phonoriton problem and discuss two

new experiments we proposed elsewhere:¹⁹ NLRBS and nonlinear modulation reflection (NLMR), which could give clear and convincing evidence of the phonoriton reconstruction.

From the previous discussion, we know that the most probable case for phonoriton reconstruction is the scattering through the LO phonon in polar semiconductors. Therefore, we will only consider the situation related to LO phonon and only anti-Stokes scattering, since experimental confirmation of the new and intensity-dependent gap is the most desirable goal. Because the IRS is phenomenologically related to phonoriton reconstruction, we also discuss its relation to the IRS experiment on exciton polariton in semiconductors.

The first paper claiming to find evidence in favor of phonoriton reconstruction appeared in 1985. Vyskovskii *et al.*¹⁷ measured the transmission spectra of CdS crystals in the presence of an intense pump light. With the

pump frequency 50 meV below the exciton energy and the pump intensity of 50 Mw/cm², they did find that the transmission coefficient K at $\omega = \omega_{\text{pump}} + 38$ meV (LO phonon) increased greatly when the pump is on. But they could not determine the details of the spectrum since the estimated new gap was about 0.3 meV, and the limit of spectral resolution of their apparatus was 0.5 meV.

Brodin, Kadan, and Matskosov¹⁸ performed a set of three photoluminescence (PL) experiments on HgI₂ crystals. The first experiment was to measure the PL spectrum of a crystal excited in the region of the excitonic absorption by a dye laser (1), in the presence of radiation from another laser (2) in the transparent region below the exciton band. They found that dip appears clearly when the laser 2 is turned on, i.e., presumably in the presence of the macropopulated polaritons. The dip shifts with the tuning of laser 2 and keeps a constant distance to the laser 2 frequency of 14.5 meV, which is the energy of the LO phonon in HgI₂ with symmetry A_{1g} . This clearly gives evidence of the formation of a new gap at the anti-Stokes frequency. In the second experiment, only laser 2 was used, and it was hoped that the Raman scattering itself would create the phonoritons. But the gap was not detected, although the anti-Stokes line existed. These authors attributed this also to the limitation of their apparatus. (Note that, at present our opinion is that this phenomenon is not only due to the limitation on resolution of the apparatus. At low temperature, the number of LO phonons is exponentially small. So the real anti-Stokes scattering is also extremely weak. Brodin observed light by increasing the intensity, thus the intensity of Stokes scattering is also increasing, and even could become stimulated scattering. The emitted phonon could be absorbed in anti-Stokes scattering, and the conservation relation cannot be satisfied by two branches of anti-Stokes scattering; thus the gap cannot be detected. Classically, this corresponds to simulated anti-Stokes scattering through Stokes–anti-Stokes coupling. We plan to discuss elsewhere the stimulated anti-Stokes scattering.)

The third experiment of Brodin, Kadan, and Matskosov, concerned the dynamical equilibrium between pump and scattered polaritons and nonequilibrium bose condensation problem. That is, there is a tendency for phonoritons to macroscopically condense to a few modes. We will not discuss this problem here.

As for IRS, most experiments carried out were related to liquids or solutions. Ishihara⁵ measured the IRS spectrum for an A_{1g} phonon in red-HgI₂ and 2H-PbI₂ single crystals. However, his main result was the presence of the inverse Raman effect: No evidence of a dynamical Stark effect was found, and the data were treated using the theory of third-order nonlinear susceptibility. It was mentioned in the paper that the linewidth of the exciton absorption in red-HgI₂ was 1.9 meV; thus we suppose that the reason why reconstruction was not observed is because of the insufficient intensity of the pump and poor quality of the sample.

Greene *et al.*⁴ observed the hole-burning effect on the exciton line in a quasi-one-dimensional semiconductor and correctly attributed this to the exciton-phonon interaction. This is also a phonoriton effect.

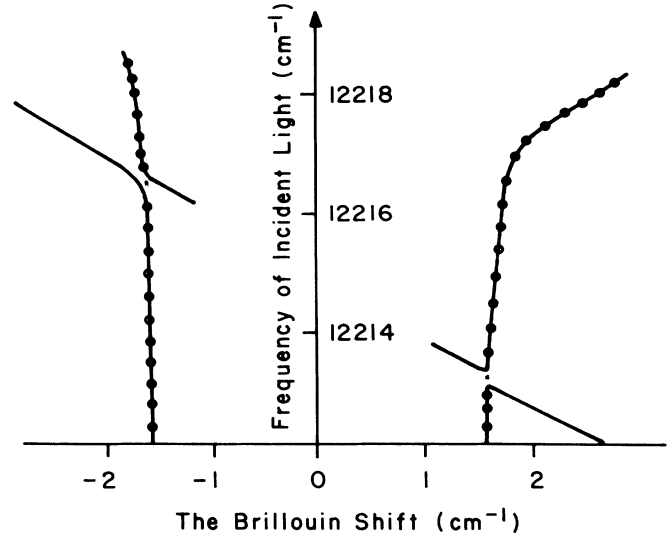


FIG. 5. The calculated Brillouin shifts of Stokes and anti-Stokes NLRBS for a phonoriton in GaAs. For pump condition, etc., see text. The continuous dotted curve is for the parent polariton.

As far as we know, the experimental evidence up to now for the phonoriton reconstruction is not very convincing and only gives a hint of possible existence of the new gap, not the basic features of elementary excitation—its dispersion relation, including the lifetime. It is therefore desirable to have more direct experimental methods to detect the phonoriton spectrum.

We now propose two modified nonlinear experiments, i.e., the RBS and the reflection spectrum; these have been proved^{21,30,31} to give very accurate information in the linear regime about the dispersion of the parent polariton, so that they can be used in the nonlinear regime. A brief report¹⁹ was already given.

A. Proposed nonlinear RBS experiment: NLRBS

The proposed modification of usual RBS for the polariton is the presence of the second pump laser beam, which provides the macropopulated polariton mode needed to produce the phonoriton reconstruction. From the previous discussion, we know that the frequency of this beam should be on the lower branch below ω_l in order to satisfy the requirement of (26). In order to simplify and clarify the problem, we suggest choosing $\omega_0 < \omega_l - \omega_{\text{LO}}$, so that only the lower branch of the polariton will be reconstructed. In the presence of the macropopulated polariton mode ω_0, \mathbf{k}_0 , the dispersion and the expected experimental results are shown in Fig. 5. Theoretically, the only difference between the two cases (with and without pump beam) is the reconstruction of the final states. Since the basic scheme is the same, we can use the results

of the theory of RBS for polariton originated by Brenig, Zeyher, and Birman, and adopted by Matsushita and co-workers^{32,33} and Tilley³⁴ with only a few modifications.

According to the RBS theory,²⁵ the integrated scattering cross section can be expressed as follows:

$$\begin{aligned} \frac{\partial \sigma_{ij}^{\text{ext}}}{\partial \Omega_j^{\text{ext}}} &= \frac{S}{(2\pi)^3 (hc)^2} T_i(\omega_I) T_j'(\omega_s) \\ &\times \frac{\omega_s^2 |\Gamma_0(K'_{ij})|^2 |A_{ij}(k_{Ii}, k_{sj})|^2}{v_{Ei}(\omega_I) v_{Gj}(\omega_s) |K''_{ij}|} \\ &\times \begin{cases} 1 + n_{\text{ph}}(\omega_I - \omega_s) \\ n_{\text{ph}}(\omega_I - \omega_s) \end{cases}, \end{aligned} \quad (47)$$

where $n_{\text{ph}}(\omega)$ is the Bose-Einstein distribution of phonons. The upper line in the curved bracket is for Stokes scattering, the lower for anti-Stokes. The subscript s stands for scattered, I for incident, and i and j denote the polariton branch under investigation. The quantity S represents the area of illumination. $T_i(\omega_I)$ is the transmissivity of the incident light (from vacuum to the sample), $T_j'(\omega_s)$ is the transmissivity of the back-scattering wave (from the sample to vacuum). These two quantities depend on the Maxwell boundary conditions, as well as the additional boundary conditions (ABC), and were extensively discussed. Here, we mention the necessary changes related to the phonoriton.

The ABC problem may be simplified since we are only concerned with a phonoriton constructed by mixing with LO phonon, which is nearly dispersionless. If we ignore the damping, there will be only one branch of the phonoriton at given frequency. If the frequency ω_s is lower than the frequency of longitudinal exciton $\omega_I(0)$, the boundary condition is the same as in local optics; if $\omega_s > \omega_I(0)$, then an additional boundary condition is needed. Of course, in each case the value of the wave vector of the phonoriton branch should be taken according to its dispersion relation.

The transmissivity $T_i(\omega_I)$ should not change. But in calculating the transmissivity $T_j'(\omega_s)$, there are two points that need special attention. First, while the outgoing scattering wave is a phonoriton, the ingoing wave with same frequency remains basically a polariton (since the momentum transfer in the forward-scattering case is much smaller than that of the back-scattering case, the spectrum reconstruction in the former case is very small and can be neglected). Since the wave vectors of this pair of waves have different values, the reflection symmetry is lifted by the pump light. Second, in determining the susceptibility, the spectrum reconstruction should be included, i.e., the exciton strength function can be viewed as the product of that function of polariton and the weight of the polariton in phonoriton Φ_{kj} , so that

$$\Phi_{kj} = \frac{1}{2} \left[1 + \frac{\frac{1}{2}[\omega_j(\mathbf{k}) - \omega_{\text{ph}}(\mathbf{k})]}{\omega_k(k) + \frac{1}{2}[\omega_j(\mathbf{k}) + \omega_{\text{ph}}(\mathbf{k})]} \right], \quad (48)$$

where $\omega_k(k)$ is the frequency of the k th branch of phonoriton, while $\omega_j(k)$ and $\omega_{\text{ph}}(k)$ are the dispersion of the polariton and phonon (here, the LO phonon).

$\Gamma_0(K'_{ij})$ in Eq. (19) is the matrix element of the exciton-phonon interaction; here it refers to LA (deformation potential interaction) and TA (piezoelectric interaction). Here the prime on the wave vector stands for the real part and double for the imaginary part. The argument K'_{ij} is the momentum transfer $K'_{ij} = K'_i - K''_j$. K''_{ij} is the uncertainty of the phonon, $K''_{ij} = K''_i + K''_j$. It also represents the linewidth of scattered light. $v_{Ei}(\omega_I)$ is the energy velocity of the mode- i polariton at frequency ω_I , v_{Gj} and (ω_{sj}) is the group velocity of the scattered wave (polariton or phonoriton). They can be calculated with standard methods.

Finally, we discuss the factor A_{ij} . It originates from the transformation from exciton to polariton and the correction Φ_{kj} of the final states which, we add, is the weight factor of the polariton in the phonoriton in the final state.

We calculated the Brillouin shifts, the linewidths, and the scattering cross sections of LA RBS for CdS and GaAs, with and without an intense pump frequency of about a LO phonon energy below the exciton resonances ω_I . The results for CdS were published earlier.¹⁹ The material parameters that we adopted are those listed in Table I. For GaAs, we choose the pump light frequency at $11\,950\text{ cm}^{-1}$ and take exciton and phonon lifetime corresponding to $\gamma_{\text{ex}} = \gamma_{\text{ph}} = 1.0\text{ cm}^{-1}$. The new gap at the anti-Stokes frequency is assumed to be 1 cm^{-1} , and the corresponding pump power density is 10 MW/cm^2 . The calculated results for Stokes and anti-Stokes cases are shown in Figs. 5–7, respectively. The Brillouin shifts for both GaAs and CdS give a clear picture of the spectrum reconstruction. However, the profile of the scattering cross sections versus frequency for GaAs is different from that for CdS, i.e., there is a lump at the photonlike part of the lower branch of the phonoriton. The reason for this is mainly the smallness of the oscillator strength of the $1s$ exciton in GaAs (ω_{1t} is only 0.08 meV), so that the resonance occurs at a very small frequency range and is steeper (also, the assumed new gap is slightly larger than ω_{1t} .) It is the resonant behavior of the exciton, the change of the group velocity, and the other factors, such as the transmission coefficients (which depend on ABC and change greatly at the resonance) that all together give the profile of the scattering cross section and linewidth. The appearance of the lump could make the determination of the phonoriton easier.

Since the intensity of the pump is high, probably the only possible way to perform the experiment is under the pulse condition. The lifetime of the polariton is presented in Sec. III. On the other hand, in order to avoid the signal from the scattering of the pump, the probe should probably also use the synchronous modulation technique.

B. Proposed nonlinear reflection experiment: NLRM

The second experiment we suggest is a reflection measurement. Assume that the pump condition is the same as that in the last experiment. In fact, Ivanov and Vygovskii¹⁵ have calculated the splitting and the modification of the exciton reflection in the presence of intense polariton waves interaction with phonon. But in

their calculation the intensity is too large, and the frequency they chose caused the spectrum change in both the upper and lower branches of the polariton, which became very complex. We choose here the pump condition, where only the lower polariton is involved, so that the analysis will be simpler. We also should emphasize the geometry of the setup: In order to get the information about the backscattering branch, the probe beam should be in the opposite direction, as shown in the upper corner of Fig. 6. Reflection can then be determined by the standard formula for reflectivity R as follows:

$$R = \left| \frac{a_1(1-n_{c2})-a_2(1-n_{c1})}{a_1(1+n_{c2})-a_2(1+n_{c1})} \right|^2. \quad (49)$$

Here, the coefficients a are given by specific ABC: We use the Pekar ABC for simplicity. Some results for CdS were published earlier.¹⁹ For GaAs the results are given in Fig. 8. We chose a different pump frequency, and the reconstruction occurred at 12210 cm^{-1} . We also changed the lifetime parameters and the gap (we took both as 0.1 cm^{-1}). In this case, the change of reflectivity $R(\omega)$ is still very prominent. Owing to the strong change

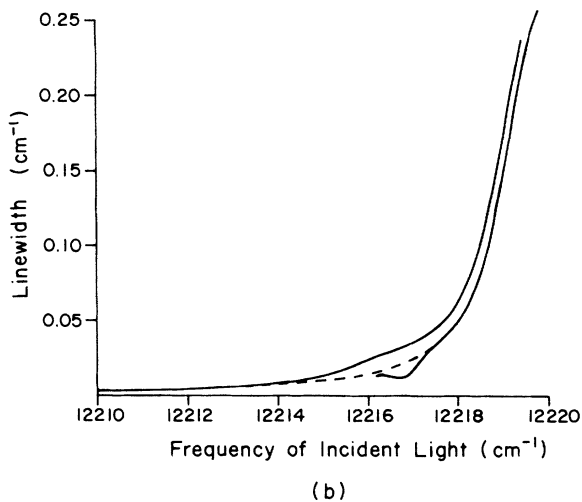
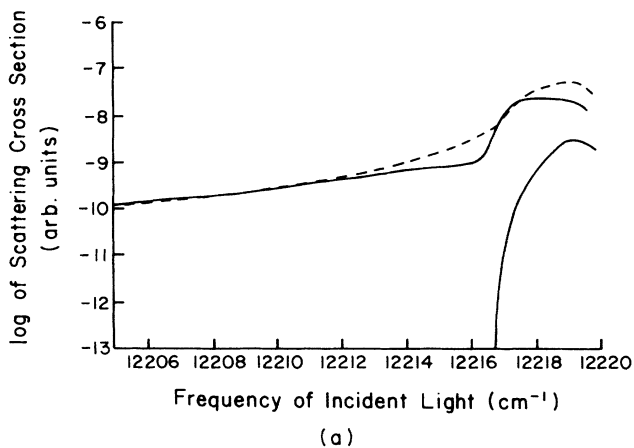


FIG. 6. (a) Predicted scattering cross section and (b) linewidths of Stokes NLRBS for phonoriton in GaAs. Parameters used are given in text. The dashed line is for parent polariton.

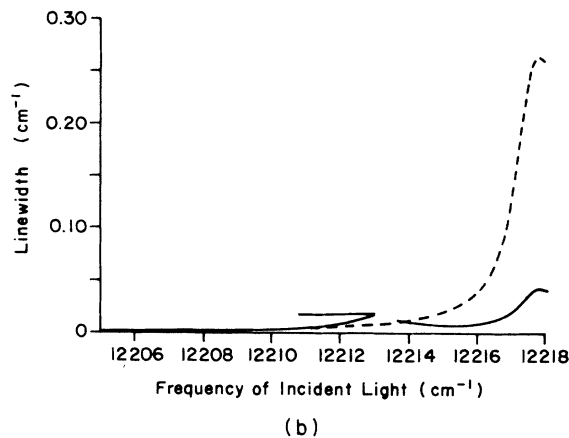
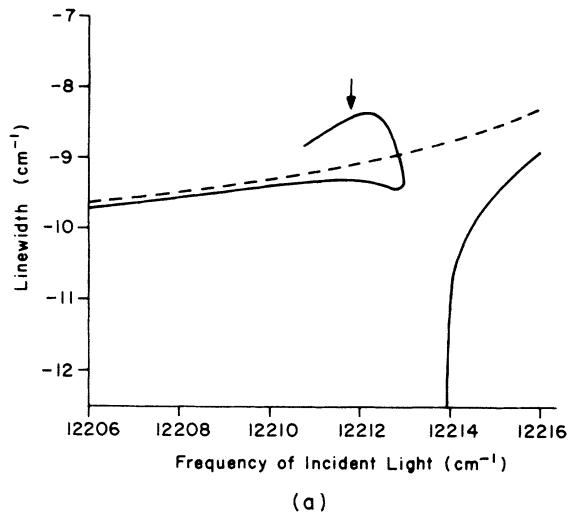


FIG. 7. (a) Predicted scattering cross section and (b) linewidth of anti-Stokes NLRBS for phonoriton in GaAs. Parameters used are given in text. For the dashed curve, see Fig. 6. Note the double values for one-incident frequency. The arrow in (a) points to the curve corresponding to the phononlike part of the lower branch of the phonoriton.

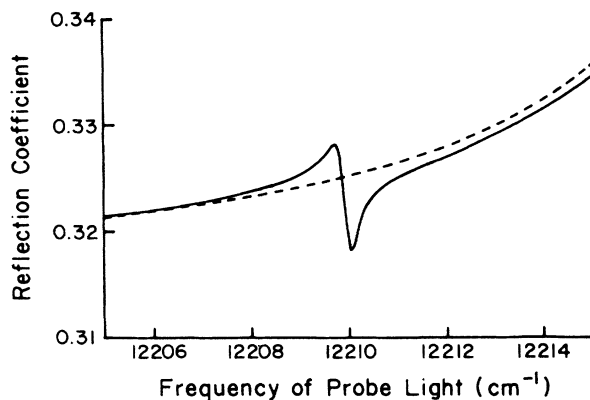


FIG. 8. Reflection spectrum of phonoriton in CdS. The solid curve is for the case $P_0=1 \text{ MW/cm}^2$. The reflection is measured in probe side (see Ref. 19). For the dashed curve, see Fig. 6.

of reflectivity $R(\omega)$ when a phonoriton is present, it may be that a nonlinear modulation spectroscopy experiment will be most appropriate to detect the effect. As mentioned before, regarding NLRBS, we suggest that in NLMR, the pulsed pump and the modulation technique should also be used.

VI. SUMMARY

We have discussed the basic concepts of the phonoriton and some of the physical consequences related to this problem. The most distinguishing feature of the phonoriton problem is that the spectrum of the quasi-particles depends on the pump level. More precisely speaking, the spectrum and occupation distribution of the quasiparticles are interrelated, as must be true in an interacting many-body system. In the ordinary low-excitation conditions, the spectrum is supposed to be fixed; then the excitation is treated as perturbation on it. In many cases, such as SRS and SBS, this approximation is also used for high-intensity excitations. The phonoriton problem, however, shows that the dynamical aspects of the spectrum cannot be neglected in high-intensity excitation,

nonlinear phenomena. More generally, the phonoriton is one kind of optical Stark effect that is currently under study. Owing to the existence of the resonant level (phonon plus polariton), the effect is easier to detect, since it needs smaller pump power than ordinary optical Stark effect. The phonoriton itself is also related to some other interesting questions, such as threshold behavior, Bose condensation, and "squeezing," because the polariton itself is intrinsically squeezed.³⁵ These problems deserve more attention, both theoretically and experimentally, and we will discuss them elsewhere.

ACKNOWLEDGMENTS

The authors would like to thank Professor L. V. Keldysh, Professor H. Z. Cummins, Professor E. Koteles, Professor M. Cardona, Professor P. Y. Yu, Professor Z. B. Su, and Dr. D. S. Chemla for helpful discussions, comments, and suggestions. This work was supported by Naval Air System Command, National Science Foundation Grant No. INT-87-14455, and Faculty Research Award Program Professional Staff Congress of CUNY.

-
- ¹S. Schmitt-Rink, D. S. Chemla, and D. A. B. Miller, *Adv. Phys.* **38**, 89 (1989).
- ²D. S. Chemla, W. H. Knox, D. A. B. Miller, S. Schmitt-Rink, J. B. Stark, and R. Zimmerman, *J. Lumin.* **44**, 233 (1989).
- ³T. Higashimura, T. Tida, and T. Komutsu, *Phys. Status Solidi (b)* **150**, 431 (1988).
- ⁴B. I. Greene, J. F. Mueller, J. Orenstein, D. H. Rapkine, S. Schmitt-Rink, and M. Thakar, *Phys. Rev. Lett.* **61**, 325 (1988).
- ⁵T. Ishihara, *J. Phys. Soc. Jpn.* **57**, 2573 (1988).
- ⁶A. L. Ivanov and B. B. Papachenko, *Pis'ma Zh. Eksp. Teor. Fiz.* **49**, 34 (1989) [*JETP Lett.* **49**, 39 (1989)].
- ⁷A. L. Ivanov and V. V. Panashchenko (unpublished).
- ⁸A. L. Ivanov and L. V. Keldysh, *Zh. Eksp. Teor. Fiz.* **84**, 404 (1982) [*Sov. Phys.—JETP* **57**, 234 (1982)].
- ⁹A. L. Ivanov and L. V. Keldysh, *Dokl. Acad. Nauk. SSSR* **264-265**, 1363 (1982) [*Sov. Phys.—Dokl.* **27**, 482 (1982)].
- ¹⁰A. L. Ivanov, *Zh. Eksp. Teor. Fiz.* **90**, 158 (1986) [*Sov. Phys.—JETP* **63**, 90 (1986)].
- ¹¹L. V. Keldysh and S. G. Tikhodeev, *Zh. Eksp. Teor. Fiz.* **90**, 1852 (1986) [*Sov. Phys.—JETP*, **63**, 1086 (1986)].
- ¹²L. V. Keldysh and S. G. Tikhodeev, *Zh. Eksp. Teor. Fiz.* **91**, 78 (1986) [*Sov. Phys.—JETP*, **64**, 45 (1986)].
- ¹³N. A. Gippius, L. V. Keldysh, and S. G. Tikhodeev, *Zh. Eksp. Teor. Fiz.* **90**, 2213 (1986) [*Sov. Phys.—JETP* **64**, 1344 (1986)].
- ¹⁴N. A. Gippius, L. V. Keldysh, and S. G. Tikhodeev, in *Laser Optics of Condensed Matter*, edited by J. L. Birman, H. Z. Cummins, and A. A. Kaplyanskii (Plenum, New York, 1988), pp. 321–329.
- ¹⁵A. L. Ivanov and G. S. Vyskovskii, *Phys. Status Solidi (b)* **150**, 443 (1988).
- ¹⁶L. V. Keldysh, *Zh. Eksp. Teor. Fiz.* **47**, 1515 (1964) [*Sov. Phys.—JETP* **20**, 1018 (1963)].
- ¹⁷G. S. Vyskovskii, G. P. Golubev, E. A. Zhukov, A. A. Fomichev, and M. A. Yaskin, *Pis'ma Zh. Eksp. Teor. Fiz.* **42**, 134 (1985) [*JETP Lett.* **42**, 164 (1985)].
- ¹⁸M. S. Brodin, V. N. Kadan, and M. G. Matsko, *Sov. Phys. Solid State* **30**, 735 (1988).
- ¹⁹Bing Shen Wang and J. L. Birman, *Solid State Commun.* **75**, 867 (1990).
- ²⁰J. J. Hopfield, *Phys. Rev.* **182**, 945 (1969).
- ²¹R. G. Ulbrich and C. Weisbuch, in *Light Scattering in Solids III*, Vol. 51 of *Topics of Applied Physics*, edited by M. Cardona and G. Gutherodt (Springer-Verlag, Berlin, 1982).
- ²²S. S. Mitra and N. E. Massa, in *Handbook on Semiconductors*, edited by W. Paul (North-Holland, Amsterdam, 1982), Vol. 1.
- ²³J. P. Wicksted, Ph.D. thesis, City University of New York, 1983 (unpublished).
- ²⁴See Ref. 21; also *Hot-Electron Transport in Semiconductors*, Vol. 58 of *Topics in Applied Physics*, edited by L. Reggiani (Springer-Verlag, Berlin, 1985).
- ²⁵W. Brenig, R. Zeyher, and J. L. Birman, *Phys. Rev. B* **6**, 4617 (1972).
- ²⁶W. J. Jones and B. D. Stoicheff, *Phys. Rev. Lett.* **13**, 657 (1964).
- ²⁷S. Saikan, N. Hashimoto, T. Kushida, and K. Namba, *J. Chem. Phys.* **82**, 5409 (1985).
- ²⁸P. L. Knight and L. Allen, *Phys. Lett.* **38A**, 99 (1972).
- ²⁹G. D. Mahan, *Many-Body Physics* (Plenum, New York, 1981), pp. 352–367.
- ³⁰R. G. Ulbrich and C. Weisbuch, *Phys. Rev. Lett.* **38**, 865 (1977).
- ³¹G. Winterling and E. Koteles, *Solid State Commun.* **23**, 95 (1977).
- ³²M. Matsushita, J. Wicksted, and H. Z. Cummins, *Phys. Rev. B* **29**, 3362 (1984).
- ³³M. Matsushita and M. Nakayama, *Phys. Rev. B* **30**, 2074 (1984).
- ³⁴D. R. Tilley, *J. Phys. C* **13**, 781 (1980).
- ³⁵M. Artoni and J. L. Birman, *Quantum Opt.* **1**, 95 (1989).